

Finite Element based Compression and Volumetric Load Analysis for Grasped Objects

Ludwig Vogt and Johannes Schilp
Department of Applied Computer Science
University of Augsburg
Augsburg, Germany
Email: {ludwig.vogt, johannes.schilp}@uni-a.de

Abstract—Grasp evaluation criteria are not only restricted to the planning stage but also while the grasp is performed and are included as optimization parameters to select a suitable grasp. For fragile objects, a strength analysis is needed to determine damages of the object through an end effector. To evaluate this criterion, the emerging residual stresses for various grasping positions must be calculated. In this work we present a Finite Element based mechanical load analysis for a set of grasping positions. Because the grasping positions have a high spatial distribution the setup is dynamic and adaptable to various input parameters. Therefore, boundary conditions are automatically set through auxiliary objects to determine the consequences of clamping forces and volumetric loads on the grasped object. Through the inclusion of all possible mechanical loads we are able to perform a fully comprehensive strength analysis. Our evaluation for a reference object showed comparable displacements ($<0.1\%$) to a manually specified strength analysis in *Ansys Structural* while significantly reducing the time to set up the strength analysis.

Index Terms—robotic grasping, mechanical load analysis, finite element analysis

I. INTRODUCTION

Traditionally most work in robotic grasping focuses on identifying a suitable grasping position and an ensuing evaluation of these positions for the grasp selection [1]. Grasp determination algorithms use different methods, e.g. the wrench space formula [2], primitive shapes [3] or clustering algorithms [4] to determine grasping positions for the combination of handling object and gripper. From these algorithms, often a sizable solution set with many possible grasps results (c.f. Fig. 1). For handling applications one appropriate position must be selected out of the solution set. Evaluation parameters, e.g., accessibility and geometrical compliance support this step to perform a ranking and optimization of the grasps [5].

To access the mechanical load and perform a strength analysis for grasp quality metrics, the resulting displacements and stresses from the handling task are needed. During the handling task not only compression forces exist from the two gripper fingers but also a volume force acts in consequence of the end tool movement and the emerging accelerations. In case of fragile geometries or if low strength materials are handled, a detailed load analysis is necessary to prevent damage of the object. If these values are not known in advance,

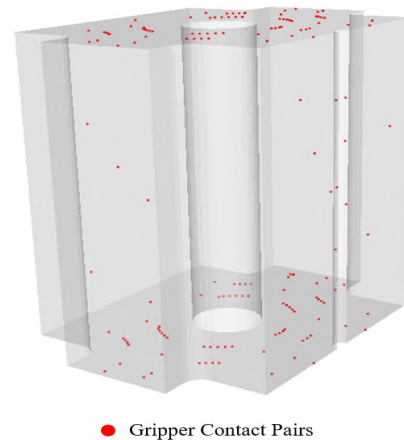


Fig. 1. 154 identified grasping positions for the reference object computed with a convex hull algorithm [8].

damage can occur during the handling task and modifications like elastic contact materials or force regulation systems [6] [7] are needed. While the Finite Element Method (FEM) is used commonly in industrial applications and many tools exist to perform load analysis, the input, environmental settings and boundary condition specifications are often set manually and require expertise from the operator. One of the main challenges is choosing the right nodes, faces and elements in the mesh for the boundary conditions because often the input data only contains sparse informations. Besides the CAD model, most of the time, only the Tool Center Point (TCP), approach vector and gripper contact points are provided in the data. To include strength analysis as a quality metric it is desired to automate the mechanical load analysis and derive all necessary information from the available data. Otherwise, evaluating all possible grasps would be exhausting and error prone if performed by hand.

To perform the mechanical load analysis we build a model which performs a compression analysis and a volumetric load analysis for a set of grasping positions and calculates the

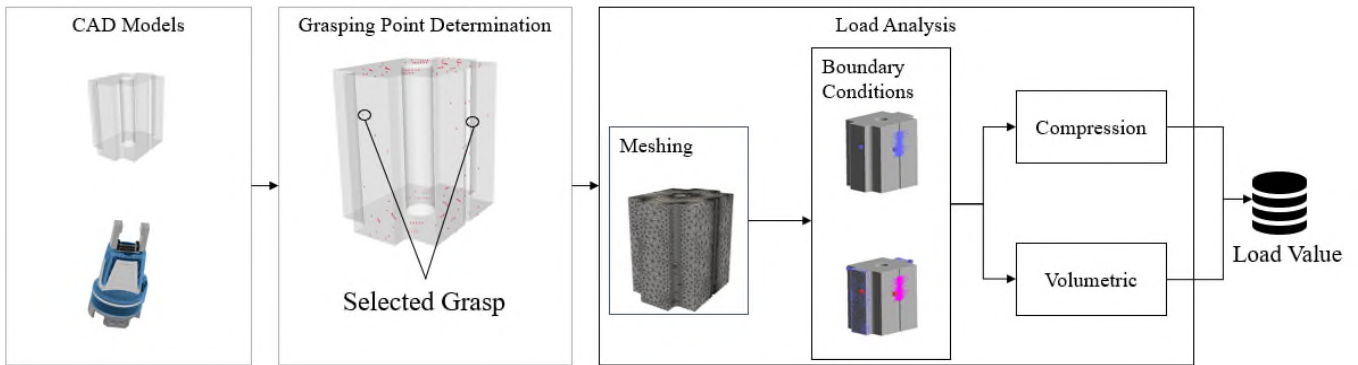


Fig. 2. Process steps of the pipeline to determine load values: 1. Importing CAD-Models 2. Grasping point determination 3. Tetrahedral meshing 4. Boundary Conditions 5 Load Analysis.

resulting displacements and stresses in the handling object. The provided data of a grasping position is enriched with a heuristic algorithm and auxiliary geometries to select suitable boundary conditions for the FEM analysis of the object. The formulation of our methods and adaption of the data enables a universal and automatic load analysis for a set of grasping positions.

The paper is organized as follows. Section II covers the past work in the fields of mechanical load analysis for robotic grasps. Afterwards, the methodology, boundary condition settings and mathematical foundation of the compression- and volumetric case are described. In Section IV we validate and show the reliability of our approach through a comparison to *Ansys Structural* for a reference object. Lastly, a summary and outlook of our work is given in Section V.

II. RELATED WORK

As a commonly used tool in many engineering applications many works already exists for the theory of the FEM and its utilization for load analysis. A good theory guide for the various steps of the numerical method is given in [9]. Therefore, in this paragraph we primary review the research concerning the load analysis in handling tasks and handling fragile objects. Many approaches use a reactive system to grasp fragile objects where the strength of the objects is not known in advance. Often tactile sensors or kinematic feedback [10] [11] are used to adapt clamping forces while grasping. A further improvement of this approach is possible through the use of depth sensors [12] and a haptic bayesian exploration. It is also possible to use a regression model [13] trained on a Neural Network with skeletal muscle information to control the force of a two fingered gripper

A mechanical orientated modeling of the contact mechanics based on the Hertzian model is used in [14] [15] [16] to model the pressure distribution in the contact plane. These models allow a detailed pressure calculation for linear and nonlinear elastic materials but only for the contact plane and not for the interior of the object.

While most quality metrics assume a rigid body and neglect failure, Pan et al. [17] first considered the effects of grasping

forces on the strength of the object prior to the handling task. Their work showed that the existing quality measures and mechanical contact models are good for predicting the stability of the grasp but not at predicting a damaging of the object. Therefore, they used the Boundary Element Method (BEM) to determine a Q_{SM} quality parameter, which specifies the mechanical load resulting from volumetric forces. Because their use of the BEM method to determine the stress field only the surface of the object can be evaluated.

III. METHODOLOGY

The load analysis (cf. Fig. 2) consists of a volumetric load analysis (cf. Section III-B) and a compression analysis (cf. Section III-C) which is performed on a precomputed grasp. We use self developed algorithms to determine different contact forms. Form closure contacts for plane contacts are determined via a polygon clipping algorithm [18] and line- or point contacts are calculated through local convex hulls [8]. To calculate form closure contacts a feature based algorithm [19] was extended to a two sided comparison. The input parameters for the FEM Analysis are derived from the grasping positions and the CAD models of the gripper and object. Input data for a single grasping position contains the stl file and the triangulated contact surfaces of the gripper. As the grasp data only contains triangulated surfaces, all additional information must be calculated from this. For this reason, prior to the FEM analysis a tetrahedral mesh is created and the stroke direction is calculated (cf. Section III-A) to determine additional information for the problem defination.

TetGen v. 0.6.0 [20] is used to create the tetrahedral meshes for the FEM analysis and for the development of the load analysis, *SfePy v. 2021.4* [21] is used as an open source package to define the FEM problem and solve the partial differential equations (PDE). In both simulations we use a Newton based nonlinear solver which utilizes a direct linear solver in every iteration.

A. Stroke Direction

A central part to derive the information for the boundary conditions is the knowledge of the stroke direction of the

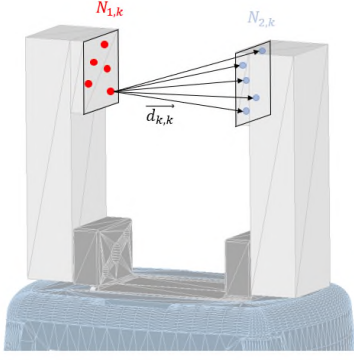


Fig. 3. Heuristic determination of the stroke direction through a connection of randomly sampled points on the gripping surfaces.

gripper, because from this vector the acceleration direction, spatial orientation of the boundary settings and the TCP can be computed. Because in our setup only the contact surface of the gripper was specified, the stroke direction \vec{s} is derived via a heuristic algorithm (cf. Fig. 3). As plane, skewed, curved and irregular shaped gripping surfaces can occur, simply calculating the vector from a pair of selected points can lead to erroneous results because the positioning of these points must be exactly antipodal.

For each gripper finger, a set of randomly distributed points on the gripping surface $N_{1,k}, N_{2,k} (k = 1, 2, \dots, z)$, where z denotes the number of points, is created. Each point in set $N_{1,k}$ is connected with all points in the antipodal set $N_{2,k}$ and the related direction vector $\vec{d}_{k,k}$ is calculated. Averaging these direction vectors for each point in $N_{1,k}$ and then over the whole set, a good approximation \vec{s} of the real stroke vector can be achieved

$$\vec{s} = \frac{\sum_{l=1}^z \sum_{k=1}^z \frac{N_{2,k} - N_{1,l}}{z}}{z}. \quad (1)$$

It is necessary to perform a vector normalization $\hat{d}_{k,k}$ of the direction vectors to neglect the length influence of individual vectors. From our testing we identified a density of 0.2 points per mm^2 for the random points to consistently get a deviation smaller than 1 % of the precise stroke direction.

B. Volumetric Load Analysis

During the handling task, the path and movements of the end tool results in different accelerations and forces on the object. As [17] showed, most algorithms simplify the force equilibrium and assume that the force is acting on the center of gravity. In reality the force acts on every part of the object so the assumption of a volumetric force is more accurate. Because there is a high variation in the direction of robotic paths we used a comprehensive method to determine a local coordinate system and the three main directions for every grip. The acceleration is superimposed with the acting gravity vector to generate 6 accelerations $a_{1..6}$ (cf. Fig. 4). Hence, the first direction equals the stroke direction \vec{s} and the second and third directions are perpendicular to each other to build

a local coordinate system. The requirement for perpendicular orientation results in one equation for direction one and two, with three unknowns x_2, y_2, z_2 for the vector of direction two

$$\cos(90^\circ) = \frac{x_1 \cdot x_2 + y_1 \cdot y_2 + z_1 \cdot z_2}{\sqrt{x_1^2 + y_1^2 + z_1^2} \cdot \sqrt{x_2^2 + y_2^2 + z_2^2}}. \quad (2)$$

Without further restrictions an infinite solution set is possible, so we set x_2, y_2 equal to 1 and solve the underdetermined equation for z_2 . The third direction is calculated via the cross product of direction one and two. After determining the accelerations, the volume vector forces \underline{f} can be calculated

$$\underline{f} = \frac{m \cdot \vec{a}}{V}, \quad (3)$$

where m denotes the mass of the object, \vec{a} the acting acceleration and V the volume of the domain. The next step includes the settings of the geometrical boundary conditions to place restrictions for the FEM formulation between the contact region of the gripper and the handling object. For the volumetric load analysis this region is fixed and has a zero displacement in every direction as it is assumed that the clamped part of the object is not moving. The relevant nodes in the mesh are selected via linear programming (LP). This algorithm evaluates, whether the nodes are inside an auxiliary geometry (cf. Fig. 4). Without an auxiliary object it is difficult to examine the nodes to fixate because the exact shape of the intersecting surface is not always known and can be difficult to determine.

For every triangle derived from the gripping surface a triangular prism is created with the selected triangle as its base and extruded towards the TCP (cf. green marked triangles in Fig. 4). Afterwards, all nodes in the mesh are checked via LP if they lie in a spanned triangular prism, which evaluates if a point can be expressed as a convex combination from the edge points of the triangle. So, a node is inside a triangular prism if a non negative solution exists for:

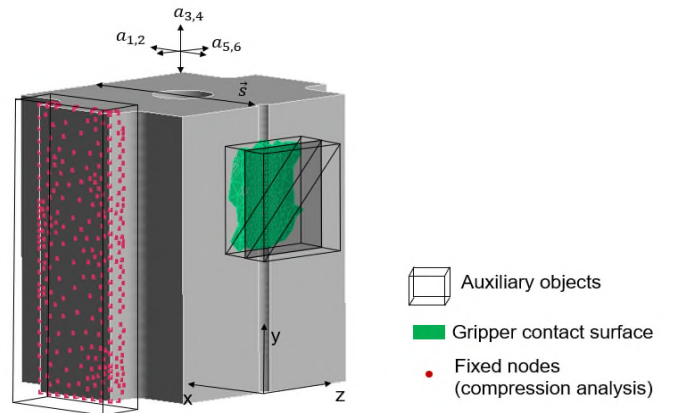


Fig. 4. Derived triangular prisms from the gripping surfaces to select the nodes for a fixed displacement at the volumetric load evaluation.

$$A \cdot \vec{x} = \vec{b}, \text{ with } x_{1,\dots,6} = 1, \quad (4)$$

where A contains the edges of the triangle and b the node coordinates. The sum of all scalar values of \vec{x} has to equal 1 to satisfy the convex point combination criteria.

As the acceleration and boundary conditions are set, the PDE for the FEM analysis can be formulated. We define, that the analysis is performed on a linear elastic material or in the linear elastic area of a material and therefore use Hooke's law for the volumetric load analysis. The PDE is derived from

$$\int_{\Omega} D_{ijkl} \cdot e_{ij}(v) \cdot e_{kl}(u) = \int_{\Omega} \underline{f} \cdot v \quad (5)$$

where Ω equals the domain of the mesh, e the cauchy strain tensor $\frac{1}{2}(\nabla u + (\nabla u)^T)$, u the displacement vector field variable, v a test function for the weak formulation of the PDE and \underline{f} a volume vector force acting on the domain. Because we assume isotropic material behavior, the stiffness matrix D for the material can formulated as followed:

$$D = \mu(\delta_{ik} \cdot \delta_{jl} + \delta_{il} \cdot \delta_{jk}) + \lambda \delta_{ij} \cdot \delta_{kl}, \quad (6)$$

where μ and λ are Lamé's coefficients derived from Young's modulus E and the Poisson ratio ν of the material. Solving this PDE in the partitioned domain yields the displacement and stress values of each node. We loop over all 6 accelerations to simulate a uniform movement and determine the resulting displacements.

C. Compression Analysis

In addition to the volumetric load, a compression force acts on the object due to the gripper. Similar to a mechanical clamp, the fingers of the gripper exert a normal force on the object. An easy way to do a compression analysis would be a comparison of the acting surface pressure of the grasp, which can be easily computed from the acting force and grasping surface, to the maximum allowable surface pressure of the material. This approach would be feasible for solid geometries, but as the clamped geometry of the object varies for each grasp, not suitable for complex geometries which contain holes or grooves.

The effective clamping forces are modeled as surface forces acting on the intersecting area between the gripper and the handling object. Similar to the volumetric case (cf. Section III-B), triangular prisms are used to identify the relevant nodes for the boundary conditions. On these nodes, the surface force f is applied. f is a scalar value, resulting from the data sheet of the Gripper which is combined with the stroke direction \vec{s} to create the acting surface forces $f_{1,2}$. While we use similar notations for the load in both cases, please note that \underline{f} represents a volume force and f a scalar force value. For the antipodal surface, the negative direction of \vec{s} is used to generate a clamping force.

Setting the boundary conditions for the compression analysis is more elaborate compared to the volumetric analysis because not all regions for the boundary conditions are specified a

TABLE I
MATERIAL PROPERTIES USED FOR THE REFERENCE CASE.

Quantity	Value [Unit]
Young's Modulus E	70 MPa
Poisson Ratio ν	0.3
Density ρ	2.7 gcm ⁻³

prior. As mentioned, only the area of the applied force can be derived directly from the contact surfaces, but the necessary restriction for the displacement needs to be defined. As the most relevant part of the object for the compression analysis lies between the two clamped surfaces, we demand that no boundary condition interferes this area. To satisfy this requirement, we use a hexahedral auxiliary geometry (cf. Fig. 4) which is shifted outside of the clamping region to select the relevant nodes. To reduce the effect of the auxiliary objects on the compression analysis, the hexahedrals are shifted as far as possible from the clamped area. Initially, the hexahedrals are positioned at the outside of the clamped area and are shifted along a vector perpendicular to \vec{s} (cf. Fig. 4) in small steps until the outside of the object is reached. At each step the nodes of the mesh are checked if they lay inside or outside the hexahedron. If the algorithm terminates, the edge of the object is reached and the antipodal side is checked whether a matching position exists. If no matching occurs, the direction is rotated around \vec{s} in small steps until a solution is found. For most objects and materials the bending at positions far away from the clamping region is negligible, therefore we fixate the selected nodes and set the displacement to zero in all directions.

With all boundary conditions specified, the PDE of the compression analysis is formulated to complete the problem definition for the FEM analysis. The PDE of the compression analysis also consists of the linear elastic term (cf. Equation 5), but instead of the volumetric force, the surface loads are balanced:

$$\int_{\Omega} D_{ijkl} \cdot e_{ij}(v) \cdot e_{kl}(u) = \int_{\Gamma_1} f_1 \cdot v + \int_{\Gamma_2} f_2 \cdot v, \quad (7)$$

where $\Gamma_{1,2}$ are the surface domains of the acting forces $f_{1,2}$.

IV. EVALUATION

In the following, we present the results of our load analysis and compare the results to a manually performed structural analysis in *Ansys Structural* [22] for a test case. The evaluation was performed on a self created test object (cf. Fig. 1) which has cooling channels in the middle and is made out of alu. The used material parameters are displayed in table I.

A Schunk Co-act EGP-C 40 (cf. Fig. 2) with planar surfaces is used which has a maximum opening of 50 mm in our configuration and a clamping force of 50 N on each side. From a set of grasps (cf. Fig. 1) one position was selected to validate our approach. To compare the results of the load analysis our test case is manually replicated in *Ansys Academic Research*

Mechanical, Release 2022.1. While the mesh can be directly imported from *TetGen*, the node ids for the regions of the corresponding boundary conditions must be offset with the value 1 to equal the same ids in *Ansys* because of the different counting methods. All displacements $u_{x,y,z}$ are calculated as a primary variable through the FEM, therefore we use this metric to compare the results of each tool. In our case stress values are not evaluated, but can be determined through the law of elasticity.

A. Results

A first inspection of the calculated displacements (cf. Fig. 5) shows the deformations at the expected positions in both cases.

To perform a more precise evaluation and validation we determined the nodal displacements in both tools and calculated the differences in each case (cf. Fig. 6 and Fig. 7). Since we use relatively small clamping forces and accelerations, a computation of the percentual differences is more convenient than absolute values. For sake of representation we only display the evaluation of one displacement direction. In the compression case, the x-direction is analyzed as it equals the direction of the clamping force and therefore the direction of the main deformation.

For the compression analysis, the displacements of nearly all nodes in the automated method were within 0.005 % of the values calculated with *Ansys*. Our evaluation showed an exponential decline in the number of nodes for an increasing difference with the displacements of most nodes being only a fraction of the maximum value.

The volumetric analysis showed similar results to the compression case with an exponential decline for increasing difference values. Maximum values for the compression case is 0.1 % and in most cases only a fraction of that (<0.04 %).

B. Discussion

While we only showed the results in the main direction of the deformation, analyzing the other directions showed similar results with differences smaller than 0.05 %.

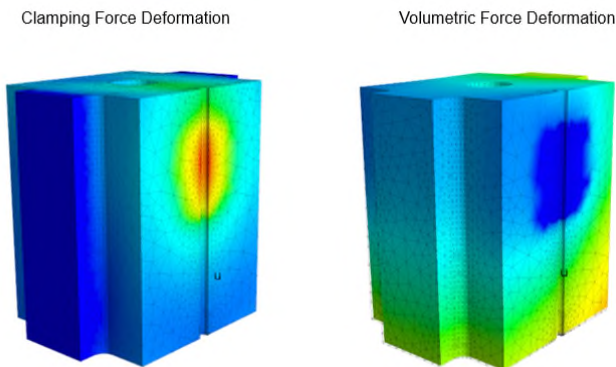


Fig. 5. Calculated displacements from the FEM analysis for the selected grasp and reference object.

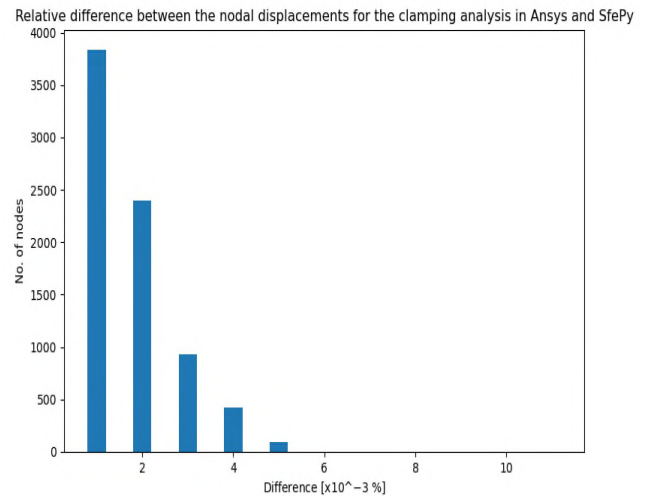


Fig. 6. Calculated relative differences between the nodal displacements for the clamping load analysis in both tools for a clamping force in x-direction. The individual differences are segmented and clustered to represent the amount of nodes with a specific difference.

maximum value of the runtime of our algorithm was less than two minutes for the reference object on a *Intel(R) Core(TM) i7* notebook processor. This included meshing the geometry, selecting and setting the boundary conditions, specifying and solving the mechanical problem and a postprocessing step. While most steps e.g., solving and meshing, take only a few seconds, the most time consuming part is the selection of the nodes, vertices and elements for the boundary conditions through the auxiliary objects. Right now this procedure takes approximately 60 % of the time. A direct time comparison to the manually performed FEM was not performed, but it can

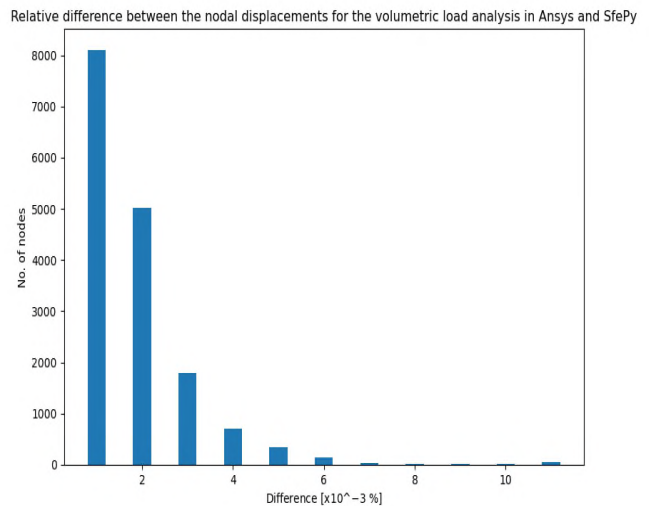


Fig. 7. Calculated relative differences between the nodal displacements for the volumetric load analysis in both tools for an acceleration in y-direction. The individual differences are segmented and clustered to represent the amount of nodes with a specific difference.

be assumed that the runtime of our algorithm is several times faster, even compared to skilled FEM operators.

V. CONCLUSION AND FUTURE WORK

In this work, we presented an approach to automatically perform a mechanical load analysis for parallel jaw grippers. The analysis includes a compression analysis in consequence of the acting normal forces and a volumetric load analysis from the resulting accelerations. The validity of our approach was shown through a comparison of the derived nodal displacements, which was in the range of 0.01 % to the calculated values of *Ansys Structural* for both cases. While the initial tests show the successful application of our algorithm a few steps can be optimized. For the development, a uniform mesh size was used which is automatically refined by *TetGen* to match the geometry of the object. The resulting refinements are not necessarily located at positions with steep displacements and therefore an offset between the numerical solution and analytical solution exists. In the future, gradient based mesh refinements [23] will be implemented to optimize the mesh in the regions with high displacements and eventually generate more accurate results. Further tests with fragile objects will be performed to validate the model in a real production environment. Additionally the stress values will be integrated in a quality metric for the grasp selection and optimization.

REFERENCES

- [1] M. A. Roa and R. Suárez, “Grasp quality measures: review and performance,” *Autonomous robots*, vol. 38, no. 1, pp. 65–88, 2015.
- [2] C. Borst, M. Fischer, and G. Hirzinger, “Grasping the dice by dicing the grasp,” in *Proceedings 2003 IEEE/RSJ International Conference on Intelligent Robots and Systems (IROS 2003) (Cat. No.03CH37453)*. IEEE, 27–31 Oct. 2003, pp. 3692–3697.
- [3] A. T. Miller, S. Knoop, H. I. Christensen, and P. K. Allen, “Automatic grasp planning using shape primitives,” in *2003 IEEE International Conference on Robotics and Automation (Cat. No.03CH37422)*. IEEE, 2003, pp. 1824–1829.
- [4] K. Harada, T. Tsuji, K. Nagata, N. Yamanobe, K. Maruyama, A. Nakamura, and Y. Kawai, “Grasp planning for parallel grippers with flexibility on its grasping surface,” in *2011 IEEE International Conference on Robotics and Biomimetics*. IEEE, 2011, pp. 1540–1546.
- [5] A. Morales, M. Prats, and J. Felip, “Sensors and methods for the evaluation of grasping,” in *Grasping in Robotics*, ser. Mechanisms and Machine Science, G. Carbone, Ed. London: Springer London, 2013, vol. 10, pp. 77–104.
- [6] M. Ciocarlie, C. Lackner, and P. Allen, “Soft finger model with adaptive contact geometry for grasping and manipulation tasks,” in *Second Joint EuroHaptics Conference and Symposium on Haptic Interfaces for Virtual Environment and Teleoperator Systems (WHC’07)*. IEEE, 2007, pp. 219–224.
- [7] Z. Hou, Z. Li, T. Fadji, and J. Fu, “Soft grasping mechanism of human fingers for tomato-picking bionic robots,” *Computers and Electronics in Agriculture*, vol. 182, p. 106010, 2021.
- [8] L. Vogt, T. Ciemala, J. Freitag, and J. Schilp, “Computing convex grasping positions for parallel jaw grippers with an integrated boundary layer mesher,” in *2021 Fifth IEEE International Conference on Robotic Computing (IRC)*. IEEE, 2021, pp. 77–81.
- [9] N. S. Ottosen, N. Saabye Ottosen, and H. Petersson, *Introduction to the finite element method*, 1st ed. New York, NY: Prentice Hall, 1992.
- [10] P. Weiner, F. Hundhausen, R. Grimm, and T. Asfour, “Detecting grasp phases and adaption of object-hand interaction forces of a soft humanoid hand based on tactile feedback,” in *2021 IEEE/RSJ International Conference on Intelligent Robots and Systems (IROS)*. IEEE, 2021, pp. 3979–3986.
- [11] H. Dang, J. Weisz, and P. K. Allen, “Blind grasping: Stable robotic grasping using tactile feedback and hand kinematics,” in *2011 IEEE International Conference on Robotics and Automation*. IEEE, 2011, pp. 5917–5922.
- [12] M. S. Siddiqui, C. Coppola, G. Solak, and L. Jamone, “Grasp stability prediction for a dexterous robotic hand combining depth vision and haptic bayesian exploration,” *Frontiers in robotics and AI*, vol. 8, p. 703869, 2021.
- [13] R. Wen, K. Yuan, Q. Wang, S. Heng, and Z. Li, “Force-guided high-precision grasping control of fragile and deformable objects using semg-based force prediction,” *IEEE Robotics and Automation Letters*, 2020. [Online]. Available: <http://arxiv.org/pdf/2002.01791v2>
- [14] N. Xydias and I. Kao, “Modeling of contact mechanics and friction limit surfaces for soft fingers in robotics, with experimental results,” *The International Journal of Robotics Research*, vol. 18, no. 9, pp. 941–950, 1999.
- [15] S. H. Bakhy, “Modeling of contact pressure distribution and friction limit surfaces for soft fingers in robotic grasping,” *Robotica*, vol. 32, no. 7, pp. 1005–1015, 2014.
- [16] P. R. Sinha and J. M. Abel, “A contact stress model for multifingered grasps of rough objects,” *IEEE Transactions on Robotics and Automation*, vol. 8, no. 1, pp. 7–22, 1992.
- [17] Z. Pan, X. Gao, and D. Manocha, “Grasping fragile objects using a stress-minimization metric,” in *2020 IEEE International Conference on Robotics and Automation (ICRA)*. IEEE, 31.05.2020 - 31.08.2020, pp. 517–523.
- [18] L. Vogt, Y. Zimmermann, and J. Schilp, “Computing gripping points in 2d parallel surfaces via polygon clipping,” in *Annals of Scientific Society for Assembly, Handling and Industrial Robotics 2021*, T. Schüppstuhl, K. Tracht, and A. Raatz, Eds. Cham: Springer International Publishing, 2022, pp. 101–112.
- [19] Y. Li, J. L. Fu, and N. S. Pollard, “Data-driven grasp synthesis using shape matching and task-based pruning,” *IEEE transactions on visualization and computer graphics*, vol. 13, no. 4, pp. 732–747, 2007.
- [20] H. Si, “Tetgen, a delaunay-based quality tetrahedral mesh generator,” *ACM Transactions on Mathematical Software*, vol. 41, no. 2, pp. 1–36, 2015.
- [21] R. Cimrman, V. Lukeš, and E. Rohan, “Multiscale finite element calculations in python using sfepy,” *Advances in Computational Mathematics*, vol. 45, no. 4, pp. 1897–1921, 2019.
- [22] “Ansys Academic Research Mechanical, Release 2022 R1, ANSYS, Inc.” 2022.
- [23] R. Moshfegh, X. Li, and L. Nilsson, “Gradient-based refinement indicators in adaptive finite element analysis with special reference to sheet metal forming,” *Engineering Computations*, vol. 17, no. 8, pp. 910–932, 2000.